Pathways to charge equilibration following multiple electron exchange between highly charged ions and atoms

de Nijs, Gerardus

Chapter 3

Experiment

3.1 Introduction

In this chapter the experimental setup will be described used in the experiments presented in this thesis. In figure 3.1 a schematic overview is presented of the KVI Atomic Physics facility. Two main parts are distinguished: firstly the source producing highly charged ions (ECRIS) and the beam line for transport of the ions (section 3.2) and in the second place the experimental setups in which different types of collisions are studied.

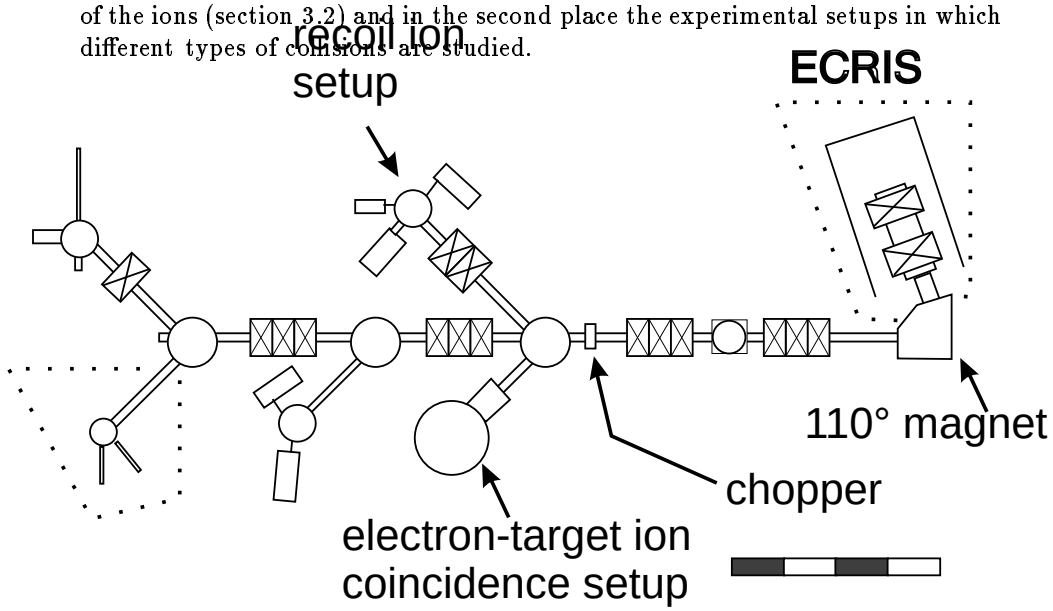

Figure 3.1: Schematic layout of the atomic physics facility

The setup for the electron-target ion coincidences (chapter 4 and 5) will be described in section 3.3. The measurements on the recoil ions, described in

chapter 6, are performed with the setup described in section 3.4

3.2 Ion beam: production and transport

Highly charged ions are produced in an electron cyclotron resonance ion source (ECRIS) installed at the KVI atomic physics facility. Ion sources of this kind can very effectively produce highly charged ions. The principle of an ECRIS is the trapping of electrons and ions in an well defined magnetic configuration. Due to the field configuration a mirror is formed: if an electron is moving along the field lines, the axial part of its velocity vector will be reversed at the high field regions in the source and will therefore be trapped in the axial direction. The radial trapping is done by a set of hexapole magnets.

Atoms are ionized in collisions with (high energy) electrons. The electrons inside the magnetic field in the ECRIS are accelerated by an RF-field which is applied to the plasma inside the source. Resonant energy transfer to the electrons is realized when the orbiting frequency of electrons around the field lines matches the frequency applied to the source.

The ion beam energy is selected by floating the source on a specific high voltage ($2 \sim 20$ kV). The ion beam extracted from the source contains all charge states created in the source. The charge state is selected by a 110° dipole magnet.

Downstream in the beam line a chopper is installed. Parallel to the ion beam two plates are mounted. The lower one is put on -150 V, while on the upper plate an alternating voltage is applied. For chopper voltages we use a square wave with top-top potential difference of 300 V. By this the beam is swept over diaphragms further on in the beam line. The ion bunches are about 50 ns wide. The chopper pulses are used to define the start of the time-of-flight measurements described in chapter 6.

3.3 Electron target-ion coincidences

After transport through the beam line the ions enter a setup in which multi-electron transfer collisions can be studied. In figure 3.2 a schematic overview is drawn. Ions enter the setup from the left. The ion beam is collimated by diaphragms and guided by a set of lenses. The ions pass through the actual reaction centre toward a Faradaycup, in which the ions are collected. The setup can be divided in two parts: in forward direction an electron spectrometer and in backward direction a target ion spectrometer. The base pressure is on the order of 10^{-5} Pa. To enhance pumping capacity, part of the setup is liquid nitrogen cooled. The reaction centre is defined as the overlap between gas target and ion beam. The gas target is formed using a conically formed gas inlet (Mack 1987). The specific form of this gas inlet guarantees an increased gas density in the reaction centre.

The reactions studied at this setup are of the form

$$\mathrm{A}^{q+} + \mathrm{B} \rightarrow \mathrm{A}^{(q-t)+} + \mathrm{B}^{r+} + (r-t)\mathrm{e}^- \qquad (3.1)$$

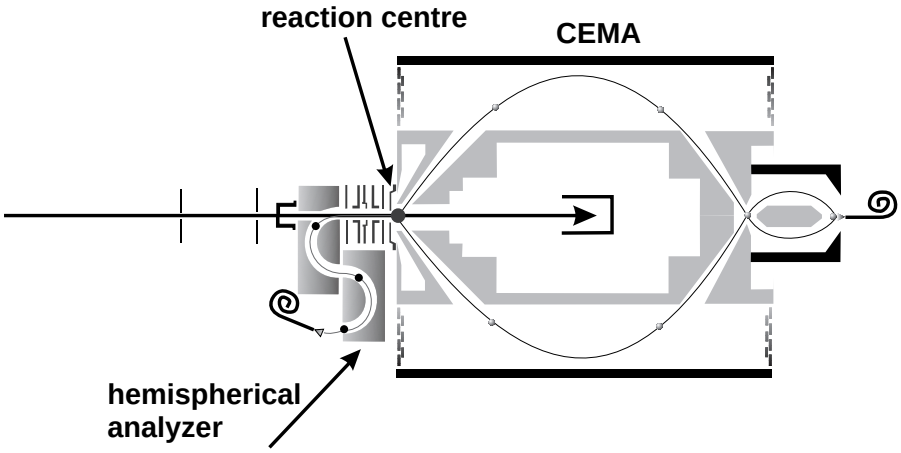

Figure 3.2: The experimental setup to measure autoionizing electrons in coincidence with the target charge state. From the left the highly charged projectile ions enter the setup. In the reaction centre the ions collide on a gas target. After the collision autoionizing electrons are detected under an angle of 50° with the beam axis with a cylindrical electrostatic mirror (CEMA) analyzer. Target ions can be detected by applying an appropriate extraction voltage on the hemispherical analyzer.

The electron capture dynamics is monitored by measuring the kinetic energy of the electrons, as well as measuring the charge state distribution B^{r+} after the collision.

In the next section the electron spectrometer is described. In section 3.3.2 the target ion spectrometer is discussed. These two are combined to measure coincidences between ejected electrons and target ions.

3.3.1 Electron spectrometer

The electron spectrometer is a cylindrical electrostatic mirror analyzer (CEMA) viewing the reaction centre under an angle of 50.0+/- 2.4° with respect to the ion beam axis. The analyzer consists basically of two coaxial cylinders. The inner cylinder is grounded, while on the outer one a voltage U_o is applied. The electric field $E(r)$ between the inner and outer cylinder at a distance r from the beam axis, is given by $E(r) = U_o[r \ln(\frac{a}{b})]^{-1}$, with a, b the radii of the inner and outer cylinder, respectively. This configuration yields an axis-to-axis focussing of charged particles (Draper and Lee 1977). Electrons of a certain energy are detected by applying the appropriate voltage on the outer cylinder. Detection is done on a channel electron multiplier (channeltron)(Philips B318BL) type detector. The head of the channeltron is put on a voltage to accelerate the electrons sufficiently before hitting the channeltron. The stray electric field due to the voltage on the head of the channeltron influences the resolution of the CEMA spectrometer. Therefore the electrons pass another small CEMA, which effectively screens the electric field.

The cylindrical symmetry of the spectrometer has as advantage that a large solid angle fraction: 3.2×10^{-2} is observed and an energy resolution of $\frac{\Delta E}{E} = 3 \times 10^{-3}$ (Mack 1987).

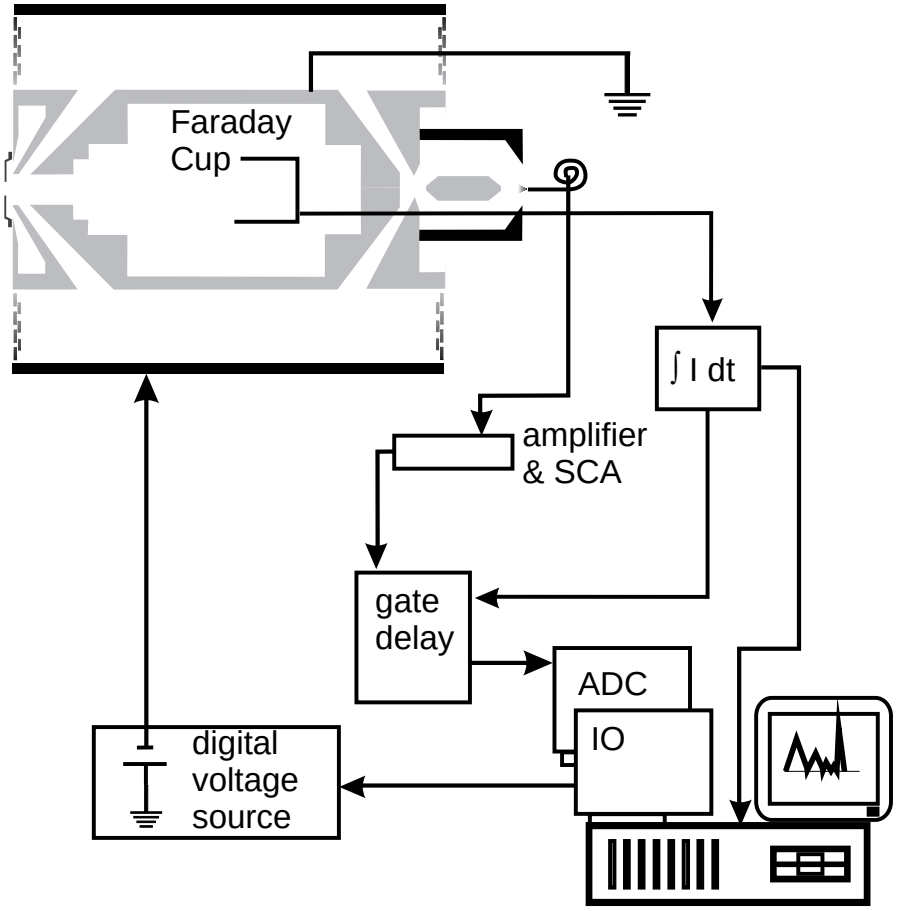

Figure 3.3: Schematic drawing of the electronics used for measuring the kinetic energy of electrons.

In figure 3.3 a schematical overview is drawn of the electronics used for measuring autoionization electrons. The signals of the channeltron are preamplified (Canberra 2004) and fed into a combined amplifier and single channel analyzer (SCA) (Ortec 690A). The output signal of this unit is used to trigger an analog to digital converter (Keithley DAS1600), which is plugged into a personal computer.

The personal computer (PC) steers the voltage on the outer cylinder. By stepping the voltage over a certain range of energies and simultaneously counting the number of events, electron spectra are measured. The voltage on the outer cylinder of the CEMA is supplied by a digital voltage source (Hewlett Packard 6131C) controlled by an PC input/output (I/O)card (Keithley PIO96).

The trigger for each voltage step is given by a counter/timer unit. The ion current in the faraday cup is integrated until a preset amount of charge is accumulated. This is measured using a programmable counter/timer (Tennelec TC512), which provides a gate signal and a trigger to the PC. At each trigger the output voltage of the digital voltage source is changed by the I/O card, in steps of 10 mV. In practice, the settings are such that approximately each 0.5 sec the voltage is changed. A sweep over the full scanning range takes about an hour.

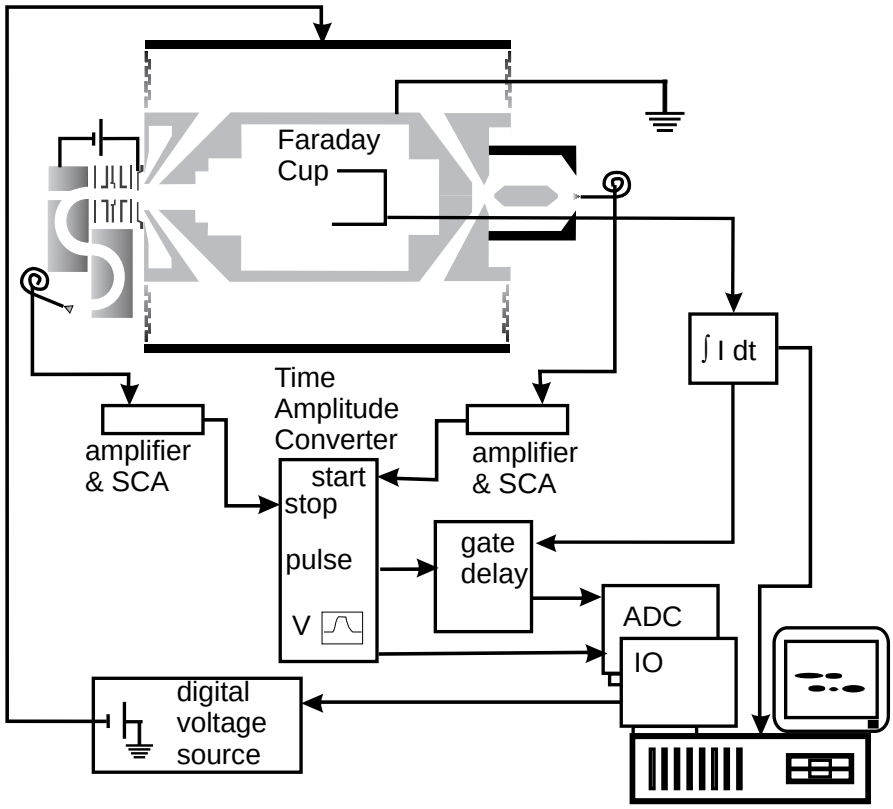

Figure 3.4: Schematical drawing of the electronics used for the coincidence measurements.

For fast measuring over the scanning range another method is used. Assuming that the ion current is constant, it is possible to generate the voltage trigger by the PC, using its internal timer. The timer generates a signal every 18.2 msec, corresponding to a frequency of 55 Hz. The timer can be modified by changing the 'divider' of the frequency generator. Writing the value 36H to I/O port 43H initiates the function to change the frequency. The next two bytes written to port 40H are the low- and high byte of the 'divider', respectively. The chosen frequency is determined by the ratio 1193180/divider. For a frequency of e.g. 75 Hz the written value should be 15909, for 1 kHz 1193 should be written to

port 40H. To restore the default value of the PC it is sufficient to write 0 to port 40H.

The software interrupt 8H, the bios timer, is called each time a trigger from the clock is generated. The bios timer controls the internal date and time of the PC and the idle time of the motor of the disks. The function of this timer can be extended by linking functions other to the software interrupt. A small procedure can be connected to the timer interrupt by calling the function `SetIntVec()`. The procedure which controls the voltage steps on the outer cylinder of the CEMA is linked to the timer interrupt. The timer interrupt has a high priority and will therefore be executed at the selected rate. In this way a 'real time' data acquisition system is constructed. The collection of data is thus separated from the steering of the setup and these two do not interfere with each other. By choosing the step frequency high enough, fast scanning over the voltage range can be realised.

3.3.2 Target-ion spectrometer

The target ions produced during collisions can be extracted from the reaction centre by applying a small extraction field (figure 3.2). The ions are guided through a couple of electrostatic lenses and are energy analyzed by means of a double hemispherical electrostatic analyzer. The hemispherical analyzer consists of an inner sphere at a negative potential and an outer sphere on a higher potential. The ions entering the spectrometer with a kinetic energy E, the 'pass energy', will pass the analyzer to a channeltron detector if the following condition for the voltages V_o and V_i, the outer and inner sphere, respectively, is fulfilled:

$$E = q(V_o - V_i)\frac{R_o R_i}{R_o^2 - R_i^2} \tag{3.2}$$

The inner diameter is $R_i = 20$ mm and the outer is $R_o = 30$ mm. During measurements the inner- and outer voltage on the spheres are fixed to -225 V and -100 eV, respectively, yielding a pass energy of 150 qV, for a given ion charge state q. Resolution is about $\frac{\Delta E}{E} = 4 \times 10^{-2}$.

3.3.3 Coincidence measurements

Coincidences between electrons and target ions are measured by scanning over the electron energy and at the same time determining the flight time of the target ions. The detection of an electron serves as a start of the time-of-flight measurements. The stop of this measurement is provided by the detection of a target ion. The average start rate is about 10 electrons per s, the stop rate ranges up to 10^4 ions per s. A schematical overview of the coincidence electronics on the setup is shown in figure 3.4.

The time-of-flight is measured by a time to amplitude converter (TAC) (Canberra 2043) by converting a time-of-flight to an output voltage. The TAC also provides a trigger pulse, which coincides with the start of the TAC output voltage pulse. The voltage is transformed to a digital value using a 16-bit ADC

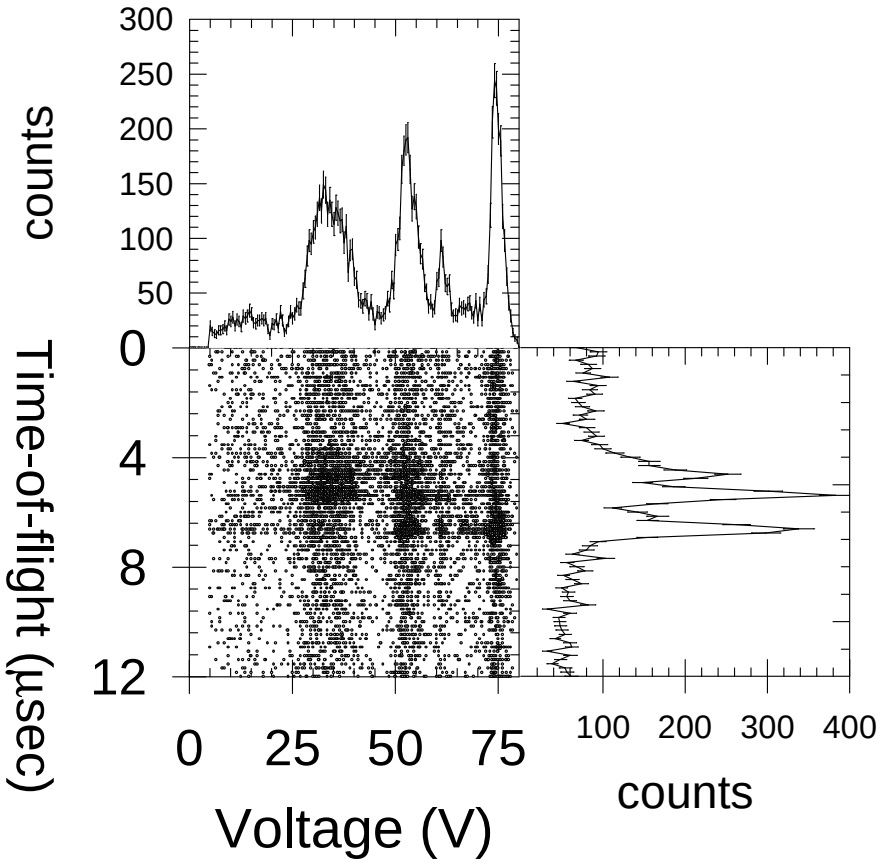

Figure 3.5: Results of a coincidence measurement before any data/background reduction. On the right of the scatterplot the total time-of-flight spectrum is plotted, on top of the figure the electron energy spectrum is drawn.

card, which can operate in two modes: a continuous scanning mode at a sample frequency of 100 kHz or in a trigger mode, where the sampling of the voltage is triggered by an external pulse. The disadvantage of the first method is that a large amount of data is generated, which has to be evaluated real time. The second method has as main disadvantage that the trigger pulse should precisely coincide with the maximum of the output pulse. Nevertheless we have chosen for the latter method, because the disadvantage can be overcome by introducing a small tunable delay to the output trigger pulse of the TAC. Such a delay is generated by the linear gate and stretcher. Another advantage of this method is that it is possible to measure current integrated. Therefore the TAC is gated by the previously mentioned counter/timer unit.

3.3.4 Data transformation and analysis

The extraction voltage on the reaction centre is chosen such that the time-of-flight of the lowest charge state of the target ions is in the order of 10 μsec. In figure 3.5 the results of coincidences between N^{7+} and Ar (see also chapter 4) are plotted. The horizontal axis is the scanning voltage, the vertical axis is the time-of-flight. An event, i.e. a measured coincidence between an electron of a certain energy and an ion with a certain time-of-flight, is indicated as a dot in the figure. The plot at the right of the graph is the sum over the electron energies, i.e. the total time-of-flight graph. The peaks indicate the different measured charge states of the target ions. On top of the coincidence figure the total electron energy spectrum is plotted. This one is obtained by summing over the time-of-flight distribution of target ions.

Electron spectra

The relation between the voltage applied to the outer cylinder U and the actual pass energy E of an electron is given by the relation $E = C * U$. For the given setup the factor $C = 1.523$ (Mack 1987). The measured electron spectra are determined in the laboratory frame. This implies that due to the moving ion the observed energies are shifted with respect to the energy of an electron emitted from an ion at rest. To compare spectra measured at different projectile velocities, the electron spectra are transformed to the emitter frame. The relation between the energy of an electron measured in the lab-(E_l) and the emitter-(E_e) frame is for a projectile energy E_{ion} given by:

$$E_e = E_l + \mu E_{ion} - 2\cos(\phi)\sqrt{\mu E_e E_{ion}} \tag{3.3}$$

where μ is the ratio between the masses of the electron and projectile: μ=m_e/m_{ion}. The angle under which the electrons are observed is ϕ. In our setup this value is ϕ=50.0+/- 2.4° (Mack 1987). The electron energy axis is corrected according to this procedure.

The observed electron yield has to be corrected for the transmission of the spectrometer and emission angle. The spectrometer operates in a $\frac{\Delta E}{E}$=constant

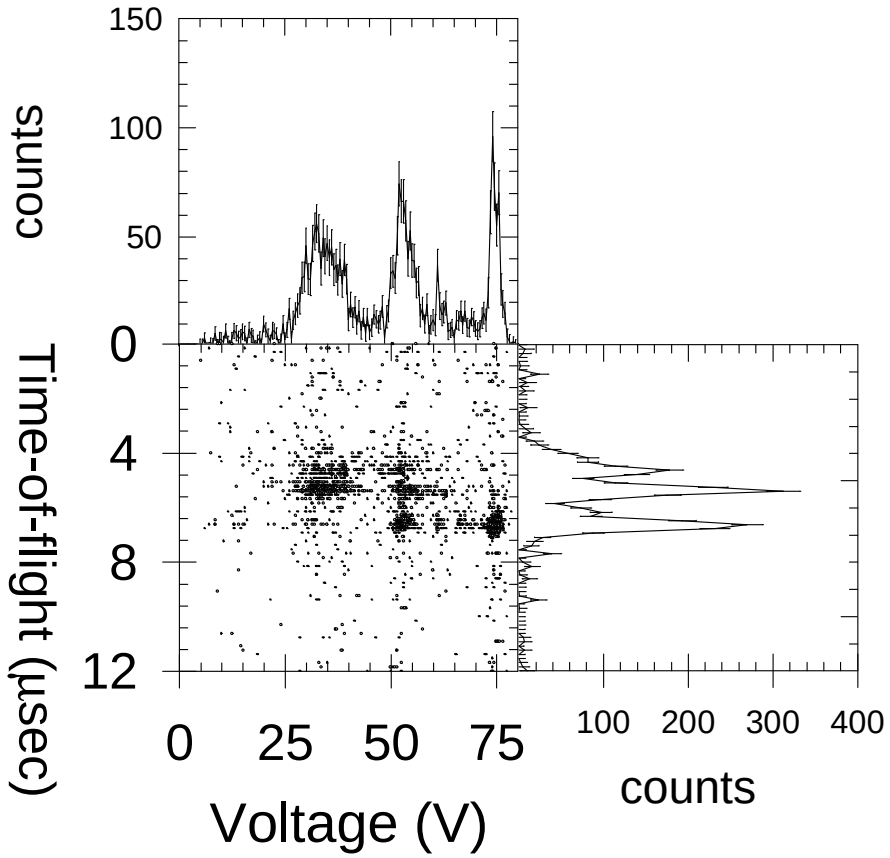

Figure 3.6: The same coincidence measurement as shown in figure 5.2 but now after the background correction procedure.

mode and therefore the observed yield at each energy E has been multiplied with a factor $\frac{1}{E}$.

Coincidences

It is clear from the sum spectrum yielding the time-of-flight graph, figure 3.5, that besides the peaks, which correspond to 'real' coincidences, a large contribution exists of background, or better, accidental coincidences. To correct the spectrum for these 'false' coincidences it is needed to perform a reliable background correction. At each electron energy a small window is set with a width of about 0.5 V. A partial time-of-flight spectrum is determined over this range. The part in which the real coincidences occur is marked. A linear background fitting procedure is then applied, but of course the part of the spectrum where the real coincidences take place is not included in the fit. This fit curve is subtracted from the total partial time-of-flight spectrum. This procedure, applied to all electron energies, yields a corrected coincidence plot as plotted in figure 3.6. After correction it is possible to extract partial electron spectra in coincidence with a charge state of the target, by applying software windows around the peaks corresponding to a charge state. After summing over all flight times of the ions in this window partial electron spectra are determined.

3.4 Reflectron

To perform high resolution analyses on the target charge state, another setup is used, which is schematically drawn in figure 3.7 (Folkerts 1996). A chopped ion beam enters the setup where it collides with a gas target. The resulting target ions are extracted by an electric field perpendicular to the beam into an ion detector. Also in this setup, the charge state of the target ions is identified by measuring the time-of-flight to a detector mounted in the apparatus. The design of this analyzer is such that time-of-flight differences between charged particles due to differences in potential are compensated. For atoms which are ionized at various places in the reaction region, the starting potential are different and thus also the flight times. It is important that time differences due to different starting positions in the extraction field are reduced. This can be done either by making the initial space distribution small compared to the distance between the extraction plates or by space focusing. To achieve space focusing together with a high mass resolution a reflecting time-of-flight spectrometer or 'reflectron' is used.

The design of the reflectron is based on the work of Karataev *et al* (1972) and Mamyrin *et al* (1973). It provides second order space focusing regarding the total time-of-flight. A schematic drawing of the reflectron is shown in figure 3.7. Consider a packet of ions with given mass and no initial energy but produced at different starting positions in the extraction field. At the end of the extraction region the ions within the packet will have different velocities due to the different starting potentials. Therefore, the packet expands during the flight through the

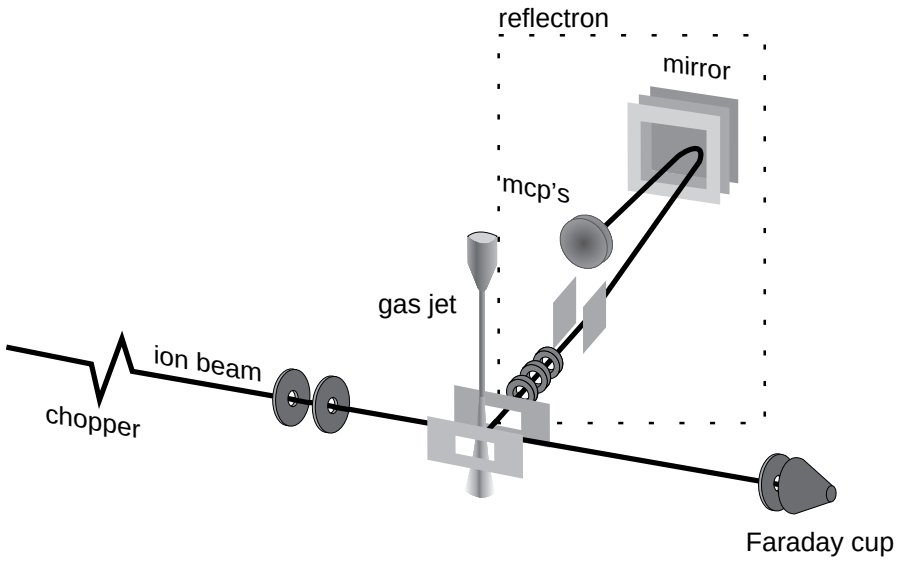

Figure 3.7: The setup to measure with high resolution recoil ion charge state distributions. From the left the highly charged projectile ions enter the setup. In the reaction centre the ions collide on a gas target. Recoil ions are extracted in a small electric field perpendicular to the projectile ion beam and are reflected in an electrostatic mirror to enhance the resolution.

spectrometer. However, after the first drift stage the ions are reflected in an electrostatic mirror. The fastest ions penetrate deeper into the mirror and spend more time in there, so the slower ions leave the mirror before the faster ones. During the second drift stage the faster ions catch up with the slower ones. With an appropriate adjustment of the parameters of the reflecting system the time interval of the packet arriving at the detector can be minimized.

References

Draper J E and Lee C Y 1977 *Rev.Sci.Instr* **48** 852
Folkerts H O 1996 Rijksuniversiteit Groningen *Thesis*
Karataev V I, Mamyrin B A, Shmikk D A and Zagulin V A 1972 *Sov. Phys. Techn. Phys* **16** 1177
Mack M 1987 Rijksuniversiteit Utrecht *Thesis*
Mamyrin B A, Karataev V I, Shmikk D A and Zagulin V A 1973 *Sov. Phys. JETP* **37** 45
Posthumus J H 1992 Rijksuniversiteit Groningen *Thesis*